

VBO-MI: A Fully Gradient-Based Bayesian Optimization Framework Using Variational Mutual Information Estimation

Farhad Mirkarimi*

Abstract

Many real-world tasks require optimizing expensive black-box functions accessible only through noisy evaluations, a setting commonly addressed with Bayesian optimization (BO). While Bayesian neural networks (BNNs) have recently emerged as scalable alternatives to Gaussian Processes (GPs), traditional BNN-BO frameworks remain burdened by expensive posterior sampling and acquisition function optimization. In this work, we propose VBO-MI (Variational Bayesian Optimization with Mutual Information), a fully gradient-based BO framework that leverages recent advances in variational mutual information estimation. To enable end-to-end gradient flow, we employ an actor-critic architecture consisting of an action-net to navigate the input space and a variational critic to estimate information gain. This formulation effectively eliminates the traditional inner-loop acquisition optimization bottleneck, achieving up to a $10^2 \times$ reduction in FLOPs compared to BNN-BO baselines. We evaluate our method on a diverse suite of benchmarks, including high-dimensional synthetic functions and complex real-world tasks such as PDE optimization, the Lunar Lander control problem, and categorical Pest Control. Our experiments demonstrate that VBO-MI consistently provides the same or superior optimization performance and computational scalability over the baselines.

1 Introduction

Bayesian optimization (BO) has matured into a de-facto tool for expensive global black-box optimization with applications in hyperparameter tuning, materials design, and experimental sciences [12, 13]. In Bayesian Optimization, the algorithm treats f as a black-box function and aims to optimize it sequentially under a finite budget T —that is, with access to only T evaluations (input–output pairs) of the function [8]. At each evaluation, the algorithm builds a probabilistic model of f , using the observed input–output pairs and uses this model to guide the selection of the next evaluation points, by maximizing a acquisition function that trades off exploration and exploitation with the goal of finding the global optimum as efficiently as possible. Traditionally, Gaussian process(GP) assumptions for the surrogate coupled

*Correspondence to: farhad.mirkarimi@mail.mcgill.ca

with various acquisition functions, such as expected improvement entropy search [17] [16], and Upper confidence bound (UCB) [41] have been effective in developing various efficient Bayesian optimization algorithms [37]. However, because standard GPs require inverting a covariance matrix (which scales cubically in the number of observations), they become computationally prohibitive for large datasets. Although approximate GPs such as sparse inducing-point models have been proposed [30], and more recent techniques based on GP approximation scale to high-dimensional BO problems [26], these methods still face trade-offs between the accuracy of finding optimal points, local fidelity, and uncertainty quantification. Recently, several works have been focused on the replacing GPs with Bayesian neural networks (BNNs) in Bayesian optimization algorithms [29, 40]. Various methods have been used in the literature for computing posteriors in the BNNs, these include variational inference with a Sparse Gaussian assumption [45], Gamma variational distribution [6], Hamiltonian Monte Carlo (HMC) among others [29]. However, all of the methods rely on the specific form of distribution for posterior sampling, which limits their capability to search entire space, specially when the underlying function is complex and high dimensional. Another limitation is computational efficiency [6] as training BNNs [29] is prohibitive.

To address these limitations, this work take a different approach and develops a framework that models the f without assuming a specific parametric family. By leveraging a flexible variational representation, the proposed approach enables more expressive uncertainty modeling and improved exploration in complex, high-dimensional search spaces. Our method enables full gradient flow through the optimization process, resulting in faster training. Specifically, we leverage recent advances in variational mutual information estimation [39, 3, 31] to design a novel acquisition function that is directly approximated from data samples. This acquisition function is jointly trained with a separate neural network, termed the action-net, which explores the input space and guides the optimization process. Our main contributions are as follows:

1. We propose a general Bayesian optimization framework that does not assume any specific variational form for the surrogate model, allowing greater flexibility in modeling complex objective functions.
2. We introduce a novel variational acquisition function (which is used as a loss function) derived from a variational mutual information formulation, which provides an explicit and principled trade-off between exploration and exploitation.
3. We provide theoretical analysis establishing the consistency and convergence properties of the proposed variational estimates and loss functions.
4. We demonstrate that our framework naturally handles noisy observations and exhibits improved robustness to the choice of the hyperparameter β compared to existing baselines.

Notation. Random vectors are denoted by bold lowercase symbols (e.g., $\mathbf{x}_t \subseteq \mathbb{R}^d$). The sequence of random vectors observed up to step t is written as $\mathbf{X}_t = [\mathbf{x}_1, \dots, \mathbf{x}_t] \subseteq \mathbb{R}^{t \times d}$. A realization (sample) of a random vector uses a superscript index (i) . Thus $\mathbf{x}_t^{(i)} \subseteq \mathbb{R}^d$, $\mathbf{X}_t^{(i)} = [\mathbf{x}_1^{(i)}, \dots, \mathbf{x}_t^{(i)}] \subseteq \mathbb{R}^{t \times d}$. Here, the index i distinguishes samples in a mini-batch or dataset.

Moreover, scalar components of a realization are written as $\mathbf{x}_t^{(i)} = [x_{1,t}^{(i)}, \dots, x_{d,t}^{(i)}]$. Calligraphic letters (e.g. $\mathcal{D} \subseteq \mathbb{R}^d$) denote domains or sets. Expectations are written as $\mathbb{E}_{P_X}[\cdot]$ under distribution P_X . The joint and product-of-marginals distributions are denoted by $P_{(X,Y)}$ and $P_X \times P_Y$, respectively. Probability density functions use lowercase notation, e.g. $p(\mathbf{x})$. Mutual information between random vectors \mathbf{X} and \mathbf{Y} is denoted $I(\mathbf{X}; \mathbf{Y})$, and $\text{KL}(P\|Q)$ denotes the Kullback–Leibler divergence between two probability measures P and Q . We use \rightarrow to denote a Markov chain.

2 Related work

The literature on Bayesian Optimization (BO) has increasingly focused on overcoming the computational limitations of traditional Gaussian Processes and application and the sampling complexity of Bayesian Neural Networks. We categorize recent advancements into three distinct research frontiers.

Scalable Bayesian optimization Gaussian Processes (GPs) remain the canonical choice for BO due to their well-calibrated uncertainty [41]. However, their $\mathcal{O}(T^3)$ complexity has led to a surge in scalable alternatives. Recent advancements include Vecchia approximations [26], which achieve linear scaling by leveraging local conditioning sets, and Trust-Region Bayesian Optimization (TuRBO) [11], which decomposes the search space into local regions to handle high-dimensional tasks. More recently, Focalized Sparse GPs [45] have been proposed to focus inducing points on promising regions of the input space. While effective, these methods often rely on stationary kernel assumptions that struggle to capture the complex, non-linear landscape of neural network landscapes.

Variational and Sampling-Based BNNs. Bayesian Neural Networks (BNNs) offer superior scalability and representation power compared to GPs. Recent efforts integrated BNNs using Hamiltonian Monte Carlo (HMC) [40, 29] for surrogate modeling of BO. To reduce the prohibitive cost of sampling, Variational Inference (VI) has emerged as a dominant paradigm. This includes the use of Variational Last Layers (VBLL) [15], which treats only the final layer stochastically, and Prior-Fitted Networks (PFNs) [33], which use Transformers to amortize the cost of Bayesian inference. Despite these gains, many VI-based BO methods still rely on specific parametric families (e.g., Gaussian or Gamma) for the posterior, which can lead to model misspecification in complex search spaces.

Information-Theoretic acquisition function desgin Information-theoretic acquisition functions, such as *Predictive Entropy Search* (PES) [18] and *Max-Value Entropy Search* (MES) [44], are prized for their principled approach to non-myopic exploration. Recent works like *Joint Entropy Search* (JES) [21] attempt to enhance robustness by modeling the joint density over optimal inputs and values; however, due to the inherent complexity of this joint density, these methods typically revert to Gaussian Process (GP) assumptions for simplification. Furthermore, recent unified framework for entropy search [6] introduce acquisition functions that lack interpretability regarding the relative contributions of exploration and exploitation due to its complexity, while being constrained by specific variational families such as the

Gamma distribution [6]. Closest to our work in spirit, [23] propose a variational lower bound maximization for entropy search. However, their formulation remains rooted in Gaussian Process framework and relies on combining over- and under-truncation approximation to maximize the bound. As it is mentioned in [23] finding a full gradient-based approach remains a open future work.

In contrast, our work reformulates the search for optimal queries as a *max-min* optimization problem, which we solve through a novel *actor-critic* inspired framework. Unlike previous work, our approach makes no Gaussian Process assumptions on f , allowing for greater expressiveness. Essentially our framework, jointly addresses the problem of uncertainty modeling and data-driven acquisition function variational mutual information estimation. We utilize two neural networks trained in an alternating, gradient-based fashion: an *actor network* (the action-net) to identify optimal inputs, and a *neural mutual information estimator* (the helper) to compute the acquisition function. By optimizing the Donsker-Varadhan variational bound through direct gradient flow, our framework eliminates the need for both the rigid kernel dependencies of GPs and the expensive posterior sampling of traditional BNNs.

3 Problem Setting and Background

We consider the task of maximizing an unknown, scalar-valued objective function $f : \mathcal{D} \rightarrow \mathbb{R}$ defined over a compact domain $\mathcal{D} \subseteq \mathbb{R}^d$. The function is a black box: its analytical form and gradients are unavailable, and each evaluation is expensive or noisy. Formally, the optimization problem is expressed as

$$\mathbf{x}^* = \arg \max_{\mathbf{x} \in \mathcal{D}} f(\mathbf{x}), \quad (1)$$

where \mathbf{x}^* denotes the global maximizer of f .

At iteration t , the optimizer selects an input \mathbf{x}_t and receives a noisy observation

$$y_t = f(\mathbf{x}_t) + \varepsilon_t, \quad (2)$$

where ε_t denotes independent, zero-mean observation noise. The history up to step t is denoted by $\mathbf{X}_t = [\mathbf{x}_1, \dots, \mathbf{x}_t]$ and $\mathbf{Y}_t = [y_1, \dots, y_t]$. Given a fixed evaluation budget T , the goal is to design a sequential policy that efficiently identifies \mathbf{x}^* using at most T steps. To assess the performance of the algorithm, we define at step t the average sum of rewards¹ as

$$S_t = \frac{1}{t} \sum_{t'=1}^t f(\mathbf{x}_{t'}), \quad t = 1, \dots, T. \quad (3)$$

3.1 Bayesian Optimization.

Bayesian Optimization (BO) addresses this problem by maintaining a probabilistic surrogate model over f and using an *acquisition function* $\alpha(\mathbf{x} \mid \mathbf{X}_t, \mathbf{Y}_t)$ to determine the next input point in T steps. Specifically, at each step next input is chosen as :

$$\mathbf{x}_t = \max_{\mathbf{x}} \alpha(\mathbf{x} \mid \mathbf{X}_{t-1}, \mathbf{Y}_{t-1}), \quad t = 1, \dots, T \quad (4)$$

¹Equivalently, the average reward normalized by the number of iterations.

At each step, BO updates the probabilistic model and chooses the next input based on previous observations up to step T . Various acquisition functions have been proposed in the literature, including Expected improvement [16], UCB [25], Entropy search [16], and [6], among others.

3.1.1 Gaussian BO

Classical BO methods employ Gaussian process (GP) surrogates, which yield closed-form posteriors and permit analytic evaluation of acquisition functions. Most prior work in the Bayesian Optimization (BO) literature [41, 27, 20, 36] explicitly assumes a particular class of black-box functions f in the underlying optimization problem. Based on these assumptions, corresponding algorithms are developed that are tailored to that class of functions. Below, we summarize some of the main assumptions commonly used in the literature:

Assumption 1. Prior assumption on f : The function $f : \mathcal{D} \rightarrow \mathbb{R}$ is assumed to be a sample drawn from a Gaussian Process (GP), denoted as

$$f \sim \text{GP}(\mu(\mathbf{x}), k(\mathbf{x}, \mathbf{x}')), \quad (5)$$

where the mean function is $\mu(\mathbf{x}) = \mathbb{E}[f(\mathbf{x})]$ and the covariance function is defined by

$$k(\mathbf{x}, \mathbf{x}') = \mathbb{E}[(f(\mathbf{x}) - \mathbb{E}[f(\mathbf{x})])(f(\mathbf{x}') - \mathbb{E}[f(\mathbf{x}')])]. \quad (6)$$

It is typically assumed that, without loss of generality, $\mu(\mathbf{x}) = 0$ and the variance of f prior is bounded, i.e., $k(\mathbf{x}, \mathbf{x}) \leq 1$ for all $\mathbf{x} \in \mathcal{D}$. In other words, for any finite collection of inputs $\{\mathbf{x}_t\}$, the corresponding (prior) function values $\{f(\mathbf{x}_t)\}$ follow a joint Gaussian distribution determined by the covariance function.

Assumption 2. Posterior assumption on f : After observing noisy samples, the posterior distribution of f conditioned on past inputs and observations remains a GP. Let $A_T = \{\mathbf{x}_1, \dots, \mathbf{x}_T\}$ denote the set of previously sampled points, where each $\mathbf{x}_t \in \mathbb{R}^d$, and $\mathbf{Y}_T = [y_1, \dots, y_T]^T$ be the vector of noisy observations, where $y_t = f(\mathbf{x}_t) + \epsilon_t$, $\epsilon_t \sim \mathcal{N}(0, \sigma^2)$ with $y_t \in \mathbb{R}$ scalar observations. It follows that the posterior distribution of f is given by [36, 41]:

$$f \mid A_T, \mathbf{Y}_T \sim \text{GP}(\mu_T(\mathbf{x}), k_T(\mathbf{x}, \mathbf{x}')), \quad (7)$$

where

$$\mu_T(\mathbf{x}) = \mathbf{k}_T(\mathbf{x})^T (\mathbf{K}_T + \sigma^2 \mathbf{I})^{-1} \mathbf{Y}_T, \quad (8)$$

$$k_T(\mathbf{x}, \mathbf{x}') = k(\mathbf{x}, \mathbf{x}') - \mathbf{k}_T(\mathbf{x})^T (\mathbf{K}_T + \sigma^2 \mathbf{I})^{-1} \mathbf{k}_T(\mathbf{x}'). \quad (9)$$

Here, $\mathbf{k}_T(\mathbf{x}) = [k(\mathbf{x}_1, \mathbf{x}), \dots, k(\mathbf{x}_T, \mathbf{x})]^T$ is the covariance vector between the new point \mathbf{x} and the previously sampled points A_T , and $\mathbf{K}_T = [k(\mathbf{x}_i, \mathbf{x}_j)]_{i,j=1}^T$ is the kernel matrix. The posterior variance at \mathbf{x} is given by $\sigma_T^2(\mathbf{x}) = k_T(\mathbf{x}, \mathbf{x})$.

3.1.2 Exploration-Exploitation trade-off

Since our goal is to maximize $f(\mathbf{x})$ with as few queries as possible, BO seeks to simultaneously approximate f globally while identifying its maximum. This corresponds to an exploration-exploitation strategy, where the approximation of the function drives the exploration, and

maximizing the acquisition function guides the exploitation. As discussed, this is done by optimizing an acquisition function, which guides the sampling of the best next query. Consider a set of input sampled points $A_T = \{\mathbf{x}_1, \dots, \mathbf{x}_T\}$, and $\mathbf{Y}_T = [y_1, \dots, y_T]$ their corresponding noisy observations, where $y_t = f(\mathbf{x}_t) + \epsilon_t$, and $\epsilon_t \sim \mathcal{N}(0, \sigma^2)$, and $\mathbf{f}_{A_T} = [f(\mathbf{x}_1), \dots, f(\mathbf{x}_T)]$ are unknown function values. We aim to choose a set of points that provides the highest possible information to approximate f , and approximate it with the fewest possible queries. To do that, the concept of information gain [41] has been used in the literature, which quantifies how much information is gained about f through observations \mathbf{Y}_T as follows:

$$I(\mathbf{Y}_T; f) = H(\mathbf{Y}_T) - H(\mathbf{Y}_T | f), \quad (10)$$

$H(\cdot)$ and $H(\cdot | \cdot)$ denote the entropy and conditional entropy. Considering the GP assumption, we have:

$$F(A_T) = I(\mathbf{Y}_T; f) = I(\mathbf{Y}_T, \mathbf{f}_{A_T}) = \frac{1}{2} \log(|\mathbf{I} + \sigma^{-2} \mathbf{K}_{A_T}|), \quad (11)$$

where $\mathbf{K}_{A_T} = [k(\mathbf{x}, \mathbf{x}')]_{\mathbf{x}, \mathbf{x}' \in A_T}$. Our goal is to select points that maximize information gain. Although finding these points among different $A \subset \mathcal{D}$, $|A| \leq T$ is NP hard, it can be done by sequentially maximizing F as follows [20, 41]:

Imagine that we have observed up to $t-1$ input points (set A_{t-1}). The optimal selection strategy for choosing the next input is such that

$$\mathbf{x}_t = \arg \max_{\mathbf{x} \in \mathcal{D}} F(A_{t-1} \cup \{\mathbf{x}\}), \quad (12)$$

In case of Gaussian assumption on f this reduces to

$$\mathbf{x}_t = \arg \max_{\mathbf{x} \in \mathcal{D}} \sigma_{t-1}(\mathbf{x}), \quad (13)$$

where σ_{t-1} is the posterior standard deviation at point \mathbf{x} after observing previous points. In next section we discuss how we will solve for exploration term to a general case other than Gaussian. Although using the strategy of using only Eq. (13) is a good way to explore globally the function, and approximate it, it is not particularly well suited to find the maximum of the function f . In this case, the objective is to [41] quickly identify locations \mathbf{x} where $f(\mathbf{x})$ attains high values, allowing the algorithm to focus sampling efforts there and effectively exploit the current knowledge. The idea is to pick points such that [41]

$$\mathbf{x}_t = \arg \max_{\mathbf{x} \in \mathcal{D}} \mu_{t-1}(\mathbf{x}), \quad (14)$$

to maximize the posterior mean of the function f so far. Based on the Gaussian assumption in [41] this term has a closed-form expression. To take into account both exploring and exploiting strategies in Eq. (13), and Eq. (14) GP-UCB rule has been applied as [41, 20, 27, 42]:

$$\mathbf{x}_t = \arg \max_{\mathbf{x} \in \mathcal{D}} \beta^{\frac{1}{2}} \sigma_{t-1}(\mathbf{x}) + \mu_{t-1}(\mathbf{x}), \quad (15)$$

where β is a constant. This sampling rule sequentially selects points \mathbf{x} such that the selected input points maximize an upper quantile of the marginal of the posterior on f up to time

$t - 1$. In other words, with high probability: $f(\mathbf{x}) \leq \beta^{\frac{1}{2}}\sigma_{t-1}(\mathbf{x}) + \mu_{t-1}(\mathbf{x})$ which accounts for choosing the name of GP-UCB bound.

However, GP-based approaches scale poorly with dimensionality and rely on Gaussian assumptions that limit their expressiveness in large data settings. Recent work [29, 40] has explored replacing GPs with Bayesian Neural Networks (BNNs) to improve scalability and representation power, using variational [45] or sampling-based posterior approximations [29].

While these methods have shown promise, they typically require strong assumptions on the posterior form (e.g., Gaussian or Gamma families) and are computationally costly [29] [6]. Moreover, as mentioned in [6], recently proposed variational acquisition functions suffer from a lack of interpretation and are too complex.

To address these limitations, we adopt a variational information-theoretic perspective that allows learning acquisition functions directly from data. without imposing explicit distributional constraints on f or the variational posterior family. We then develop a variational acquisition function (which is used as a loss function in our framework) that has each of its terms interpretable and has trade-offs between the exploration and exploitation capabilities of our algorithm without the limiting Gaussian process assumption in previous works .

4 Proposed Bayesian Optimization Framework with Variational MI Estimation

To develop our framework, Our first observation is that the policy described in Eq. (15) implicitly depends on the MI between the unknown function f and the observed rewards \mathbf{y}_t , conditioned on the selected actions \mathbf{x}_t , as established in Eq. (13) and Eq. (15). In the following sections, we leverage the results of [3] to derive a variational bound on the exploration term in Eq. (15). We then introduce a data-driven approach for estimating the exploitation term. Building on these two components, we design a loss function that enables the joint training of two Neural Networks aimed at solving our Bayesian Optimization problem: one network responsible for identifying promising actions, and a second auxiliary (helper) network that estimates information gain and provides guidance for training both models that are trained in alternative fashion.

4.1 Variational Mutual Information

To incorporate Mutual Information (MI) into our optimization strategy without relying on restrictive assumptions (e.g., Gaussianity), we employ a variational lower bound based on the Donsker–Varadhan (DV) representation [3, 10] of the Kullback–Leibler (KL) divergence.

Let P and Q be two probability measures over the same measurable space. The DV representation expresses the KL divergence as

$$D_{\text{KL}}(P \parallel Q) = \sup_T \mathbb{E}_P[T] - \log \mathbb{E}_Q[e^T], \quad (16)$$

where the supremum is taken over all measurable functions T such that the expectations are finite [3, 10]. Now, consider random variables \mathbf{X} and \mathbf{Y} with joint distribution $P_{(\mathbf{X}, \mathbf{Y})}$, and

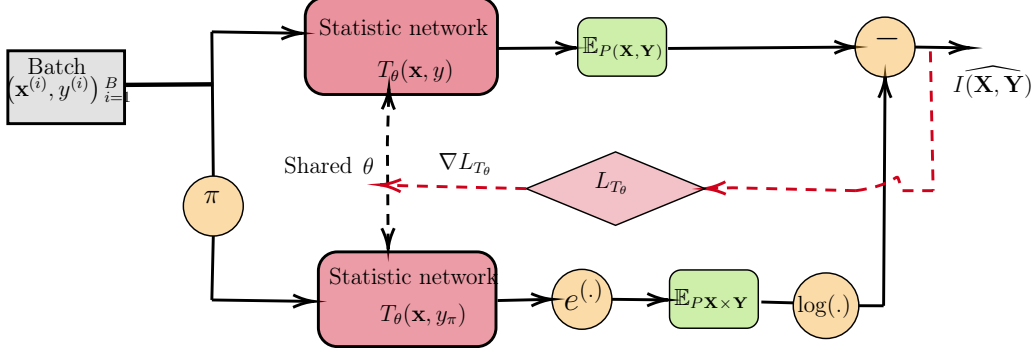


Figure 1: NN architecture for evaluating MI from samples of two distributions. Using the network output and Eq. (20), an estimate of Mutual Information is computed.

let $Q = P_{\mathbf{X}} \times P_{\mathbf{Y}}$ denote the product of marginals. Then, the MI between \mathbf{X} and \mathbf{Y} can be written as

$$I(\mathbf{X}; \mathbf{Y}) = D_{\text{KL}}(P_{(\mathbf{X}, \mathbf{Y})} \parallel P_{\mathbf{X} \times \mathbf{Y}}) = \quad (17)$$

$$\sup_{T \in \mathcal{T}} \mathbb{E}_{P_{(\mathbf{X}, \mathbf{Y})}}[T(\mathbf{X}, \mathbf{Y})] - \log \mathbb{E}_{P_{\mathbf{X}} \times P_{\mathbf{Y}}}[e^{T(\mathbf{X}, \mathbf{Y})}]. \quad (18)$$

In practice, we parameterize $T(\mathbf{X}, \mathbf{Y})$ using a Neural Network $T_{\theta}(\mathbf{X}, \mathbf{Y})$ with parameters θ , and estimate the expectations via sampling. This yields the following variational lower bound:

$$I(\mathbf{X}; \mathbf{Y}) \geq \max_{\theta \in \Theta} \mathbb{E}_{P_{(\mathbf{X}, \mathbf{Y})}}[T_{\theta}(\mathbf{X}, \mathbf{Y})] - \log \mathbb{E}_{P_{\mathbf{X}} \times P_{\mathbf{Y}}}[e^{T_{\theta}(\mathbf{X}, \mathbf{Y})}]. \quad (19)$$

Given a samples of distributions $\{(\mathbf{X}^{(i)}, \mathbf{Y}^{(i)})\}_{n=1}^N$, the Neural Network $T_{\theta}(X, Y)$ is trained by minimizing the following loss function:

$$L(\theta) = -\frac{1}{B} \sum_{i=1}^B T_{\theta}(\mathbf{X}^{(i)}, Y^{(i)}) + \log \left(\frac{1}{B^2} \sum_{i=1}^B \sum_{j=1}^B e^{T_{\theta}(\mathbf{X}^{(i)}, Y^{(j)})} \right), \quad (20)$$

where B denotes the minibatch size. This formulation provides a scalable, sample-based estimator of MI, and integrate into our Bayesian Optimization framework to guide exploration. In Fig.1 we illustrate this concept visually.²

4.2 Exploration and Mutual Information Estimation

Using these results, our goal here is to find a variational bound for exploring the function f . Based on the defined setting, at time step t we have access to $\mathbf{X}_t = [\mathbf{x}_1, \dots, \mathbf{x}_{t-1}, \mathbf{x}_t]$. Also, consider that these actions are chosen according to $P_{\mathbf{X}_t}$. Moreover, corresponding observations are $\mathbf{Y}_t = [y_1, \dots, y_t]$, where $y_t = f(\mathbf{x}_t) + \epsilon_t$, and ϵ_t is zero mean, independent,

²There are several neural mutual information methods proposed in the literature that each of them have their own limitation, and strength and work under various restrictive assumptions[34][35][43][32]

identically distributed (i.i.d.) noise. Our goal in this section is to find a lower bound on the information gain quantity which corresponds to the exploration term in Eq. (15), which is:

$$I_G = I(f(\mathbf{X}_t), \mathbf{Y}_t), \quad (21)$$

where we have³ $\mathbf{Y}_t = f(\mathbf{X}_t) + \mathcal{E}_t$, $\mathcal{E}_t = [\epsilon_i]_{i=1}^t$, and $f(\mathbf{X}_t) = [f(\mathbf{x}_i)]_{i=1}^t$.⁴ To find a simple bound on this quantity using the bound of [3], and Eq. (18), we first note that we have the following Markov chain [7]:

$$\mathbf{X}_t \longleftrightarrow f(\mathbf{X}_t) \longleftrightarrow \mathbf{Y}_t. \quad (22)$$

Based on the data-processing inequality [7] we have

$$I(\mathbf{X}_t, \mathbf{Y}_t) \leq I_G = I(f(\mathbf{X}_t), \mathbf{Y}_t). \quad (23)$$

On the other hand, by using the variational representation in Eq. (16):

$$\begin{aligned} I_\theta(\mathbf{X}_t, \mathbf{Y}_t) &= \sup_{\theta \in \Theta} \mathbb{E}_{P(\mathbf{X}_t, \mathbf{Y}_t)} [T_\theta(\mathbf{X}_t, \mathbf{Y}_t)] + \\ &\quad \log(\mathbb{E}_{P_{\mathbf{X}_t} \times P_{\mathbf{Y}_t}} [e^{T_\theta(\mathbf{X}_t, \mathbf{Y}_t)}]). \end{aligned} \quad (24)$$

By noting that $I_\theta(\mathbf{X}_t, \mathbf{Y}_t) \leq I(\mathbf{X}_t, \mathbf{Y}_t)$, and combining Eq. (23) and Eq. (24) we have the following bound on the exploration term, or IG bound in Eq. (15):

$$\mathbb{E}_{P(\mathbf{X}_t, \mathbf{Y}_t)} [T_\theta(\mathbf{X}_t, \mathbf{Y}_t)] + \log(\mathbb{E}_{P_{\mathbf{X}_t} \times P_{\mathbf{Y}_t}} [e^{T_\theta(\mathbf{X}_t, \mathbf{Y}_t)}]) \leq I_G. \quad (25)$$

In the next part, we define a loss function and state our main algorithm for Bayesian Optimization.

4.3 Loss Function and Algorithm

In this section, we develop our proposed variational acquisition function, and our proposed algorithm based on that to find best possible inputs in each step of algorithm. More specifically, we aim to solve the Bayesian Optimization problem described in Eq. (1) in T steps. To do so, we find the best possible actions for f based on maximizing an acquisition function (as a loss of neural network as described later), which we call g , through the following optimization problem:

$$\mathbf{X}_t = \max_{\mathbf{X}_{t-1}(\phi)} \min_{\theta} g(\phi, \theta). \quad (26)$$

Where ϕ , and θ_2 represent parameters of two neural networks. These two networks are trained in an alternative manner (similar to adversarial neural network) to predict next action using g using gradient descent. In what follows, we specify g , the loss function (which plays the role of acquisition function) for our neural networks using the results from the previous section. To best of our knowledge, this is the first work in this area that applies variational formulations to design a fully gradient-based Bayesian Optimization framework using deep

³Depending on its argument, f represents a scalar value, $f(\mathbf{x}_t)$ or a vector, $f(\mathbf{X}_t)$.

⁴Note that here we don't have a Gaussian assumption (for f or noise), and therefore we cannot use the closed form for Gaussian distribution entropy)

learning to extend earlier works which rely on the Hamiltonian Monte Carlo sampling (using BNNs) to high-dimensional data and settings beyond the Gaussian assumption.

To find the appropriate loss function to choose the best actions to approximate and maximize f , our loss function should simultaneously consider the balance of exploration and exploitation in searching the input space. In the previous subsection, we have seen how the information gain quantity can be leveraged to consider the exploration of the input space. To account for the exploration of our algorithm, we need to consider finding the maximum of f by exploiting our current knowledge. A straightforward approach to find the maximum is to consider the expectation of the function f conditioned on previous points (posterior of f), e.g:

$$\mathbb{E}[f \mid y_{t-1}, \dots, y_1, \mathbf{x}_{t-1}, \dots, \mathbf{x}_1]. \quad (27)$$

Furthermore, we note that by assuming that f and noise are independent, and noise has a zero mean, we have:

$$\mathbb{E}[f \mid y_{t-1}, \dots, y_1, \mathbf{x}_{t-1}, \dots, \mathbf{x}_1] = \quad (28)$$

$$\mathbb{E}[f + \epsilon_t \mid y_{t-1}, \dots, y_1, \mathbf{x}_{t-1}, \dots, \mathbf{x}_1] = \quad (29)$$

$$\mathbb{E}[y_t \mid y_{t-1}, \dots, y_1, \mathbf{x}_{t-1}, \dots, \mathbf{x}_1]. \quad (29)$$

By combining the exploitation term in Eq. (25), and exploitation in term in Eq. (29):

$$g_{\phi, \theta}(\mathbf{X}_t, \mathbf{Y}_t) = \mathbb{E}[y_t \mid y_{t-1}, \dots, y_1, \mathbf{x}_{t-1}, \dots, \mathbf{x}_1] + \quad (30)$$

$$\sqrt{\beta} \left[-\mathbb{E}_{P(\mathbf{x}_t, \mathbf{y}_t)}[T_{\theta_2}(\mathbf{X}_t, \mathbf{Y}_t)] + \log(\mathbb{E}_{P_{\mathbf{X}_t} \times P_{\mathbf{Y}_t}}[e^{T_{\theta_2}(\mathbf{X}_t, \mathbf{Y}_t)}]) \right], \quad (31)$$

where β is a constant that controls the trade-off between exploration and exploitation. As the search space \mathcal{D} for actions can be large or high-dimensional, and the function f can be non-linear and hard to approximate, we use the expressive power of NNs to solve this problem.

First, consider a neural network that searches in the input domain \mathcal{D} and outputs the desired actions (we call this network \mathbf{E} , which plays the role of encoder in our framework) :

$$E_{\phi}(\mathbf{s}_t) = \mathbf{x}_t, \quad (32)$$

where $\mathbf{s}_t = \{s_t^{(i)}\}_{i=1}^B$ is random seed vector at time step t , and $\mathbf{x}_t = \{\mathbf{x}_t^{(i)}\}_{i=1}^B$. By adding \mathbf{x}_t to \mathbf{X}_{t-1} we form \mathbf{X}_t , and by using it and output of black-box function, \mathbf{Y}_t we train a network, called "helper", which is denoted as D_{θ} to output information gain :

$$L_{D_{\theta}}(\mathbf{X}_t, \mathbf{Y}_t) = \quad (33)$$

$$-I_{\theta}(\mathbf{X}_t, \mathbf{Y}_t) = -\mathbb{E}_{P(\mathbf{x}_t, \mathbf{y}_t)}[D_{\theta}(\mathbf{X}_t, \mathbf{Y}_t)] + \quad (34)$$

$$\log(\mathbb{E}_{P_{\mathbf{X}_t} \times P_{\mathbf{Y}_t}}[e^{D_{\theta}(\mathbf{X}_t, \mathbf{Y}_t)}]). \quad (35)$$

After computation of $I_{\theta}(\mathbf{X}_t, \mathbf{Y}_t)$, this term is used in the following loss function to train E_{ϕ} , and choose the next set of actions:

$$L_{E_{\phi}}(\mathbf{X}_t, \mathbf{Y}_t) = \mathbb{E}[y_t \mid y_{t-1}, \dots, y_1, \mathbf{x}_{t-1}, \dots, \mathbf{x}_1] - \quad (36)$$

$$\sqrt{\beta} \mathbb{E}_{P(\mathbf{x}_t, \mathbf{y}_t)}[D_{\theta}(\mathbf{X}_t, \mathbf{Y}_t)] + \log(\mathbb{E}_{P_{\mathbf{X}_t} \times P_{\mathbf{Y}_t}}[e^{D_{\theta}(\mathbf{X}_t, \mathbf{Y}_t)}]), \quad (37)$$

Algorithm 1 Variational Bayesian Optimization with Mutual Information (VBO-MI)

Input: Initialized weights of networks E_ϕ (action-network (Main)) and D_θ (MI network-Helper), initial random seed \mathbf{s}_0 from a standard Gaussian distribution, number of warm-up steps W , number of BO iterations T , iteration counts K_a and K_b , batch size B .

Output: Optimized weights of E_ϕ and D_θ , estimated optimum \mathbf{x}^* .

```

1: Warm-up Phase:
2: for  $k = 1, \dots, W$  do
3:   Sample actions  $\mathbf{x}^{(i)} \sim E_\phi(\mathbf{s}_0)$ ,  $i = 1, \dots, B$ .
4:   Evaluate observations  $y_t^{(i)} = f(\mathbf{x}^{(i)}) + \epsilon^{(i)}$ .
5:   Compute  $-\text{MI}$  using  $(\mathbf{x}^{(i)}, y^{(i)})_{i=1}^B$ .
6:   Update  $D_\theta$  via gradient descent, keeping  $E_\phi$  fixed.
7: end for
8: Main VBO-MI Phase:
9: for  $t = 1, \dots, T$  do
10:  Sample a batch of actions  $\mathbf{x}_t^{(i)} \sim E_\phi(\mathbf{s}_t)$ ,  $i = 1, \dots, B$ . Concatenate  $\mathbf{x}_t \subseteq \mathbb{R}^{B \times d}$  to  $\mathbf{X}_{t-1}$  to form  $\mathbf{X}_t$ .
11:  Evaluate corresponding observations  $y_t^{(i)} = f(\mathbf{x}_t^{(i)}) + \epsilon^{(i)}$ ,  $i = 1, \dots, B$ , to form  $\mathbf{y}_t \subseteq \mathbb{R}^{B \times 1}$ , Concatenate  $\mathbf{y}_t$  to  $\mathbf{Y}_{t-1}$  to form  $\mathbf{Y}_t$ .
12:  Update  $D_\theta$  (Helper / MI Network):
13:  for  $k = 1, \dots, K_a$  do
14:    Update  $D_\theta$  by gradient descent on  $L_{D_\theta}$  with  $E_\phi$  fixed.
15:  end for
16:  Update  $E_\phi$  (Action (Main) Network):
17:  for  $k = 1, \dots, K_b$  do
18:    Update  $D_1$  by SGD on  $L_{E_\phi}$  with  $D_\theta$  fixed.
19:  end for
20: end for
21: Return: final networks  $(E_\phi, D_\theta)$  and estimated optimum  $\mathbf{x}^* = \arg \max_{\mathbf{x}} D_1(\mathbf{x})$ .

```

where the weights of θ are frozen. As these losses only have expectation terms, they can be implemented using averages over corresponding distributions. Specifically:

$$L_{E_\phi} = \frac{1}{B} \sum_{i=1}^B y_t^{(i)} - \frac{1}{B} \sum_{i=1}^B D_\theta(\mathbf{X}^{(i)}, \mathbf{Y}^{(i)}) + \quad (38)$$

$$\log \frac{1}{B^2} \sum_{i=1}^B \sum_{j=1}^B e^{D_\theta(\mathbf{X}^{(i)}, \mathbf{Y}^{(j)})}, \quad (39)$$

where $y_t^{(i)} = f(\mathbf{x}_t^{(i)}) + \epsilon_t$.

Now we resort to the loss functions L_{E_ϕ} and L_{D_θ} , and the outputs of D_1 and D_2 , to propose our algorithm for the Bayesian Optimization problem. In our framework, the E_ϕ has main responsibility for searching in the input action space \mathcal{D} , to choose \mathbf{X}_t , and the other called "helper", D_θ (with parameters θ_2) such that computes our information gain term. So, based on this loss function, we train two separate neural networks simultaneously:

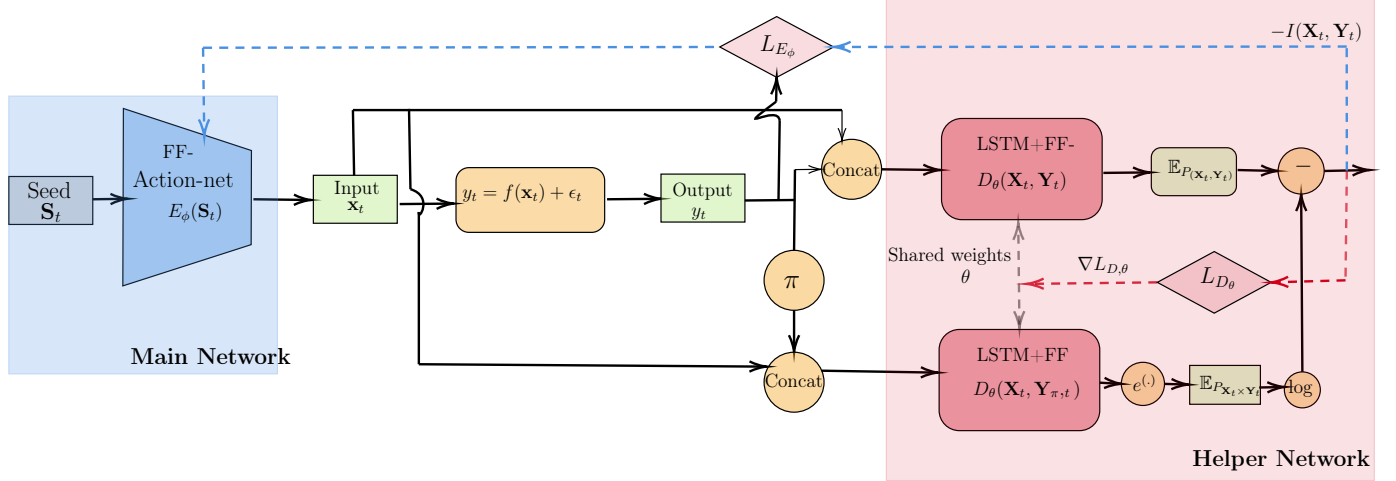


Figure 2: An illustration of the neural architecture of the proposed algorithm. Each dashed line shows the flow of gradients for training the weights of the action-net (main) and helper networks. Concat and shuffle (π) blocks are used to produce the joint and product of marginal samples to feed the helper network.

1. The D_2 , helper network, performs current evaluation of selected actions \mathbf{X}_t at time step t with corresponding observations \mathbf{Y}_t .
2. Using the information gain and L_{E_ϕ} , the E_ϕ is trained such that it can find the best possible actions to maximize our black box function f (see Fig. 2 for a complete representation of the algorithm). We use Long-Short-Term Memory neural networks and feed-forward neural networks as the architectures for D_2 , and D_1 respectively.

Our detailed algorithm for training our networks is summarized⁵ in Algorithm 1.

5 Numerical evaluation

In this section, we present numerical evaluations of our proposed method, Variational Bayesian Optimization (VBO), and compare its performance with several baselines [29, 45]. These baselines include the following methods for Bayesian neural networks: Laplace Linear Approximation (LLA) [22, 29], Hamiltonian Monte Carlo (HMC) [24, 29], Stochastic Gradient Hamiltonian Monte Carlo (SGHMC) [5, 29], Deep Kernel Learning (DKL) [46, 29], Infinite-width Bayesian neural networks (IBNN) [28, 29], and Gaussian Processes (GPs) [38, 29]. In addition, we include the focal Sparse Gaussian Process method [45] as a recent baseline for comparison with our approach.

We present our experiments on two settings. First, we test our algorithm and other baselines on a set of synthetic data and functions. Next, we consider 4 different real-world tasks, and functions similar to previous works [29, 9]. Specifically, we consider partial differential equation optimization, Interferometer position optimization, the Lunar lander

⁵We use a modified LSTM unit in our algorithm, which is explained in the remark.

game, and the pest control problem. The details and explanations regarding each task have been provided in the Appendix.

5.1 Synthetic functions

Our primary experimental setting for synthetic functions involves evaluating our algorithm on three widely used benchmark functions: Branin, Hartmann, and Ackley [29, 11]. These functions are highly nonconvex and contain multiple local optima and are therefore considered challenging benchmarks for optimization. Since these functions have global minima, and are conventionally used in minimization problems, but our algorithm is designed for maximization, we optimize $-f$ instead of f . In other words, maximizing $-f$ is equivalent to minimizing f , which allows a consistent comparison with prior work[29].

In Fig.3a, we test the baselines versus our proposed method over various test functions and baselines on the Branin test function. In Fig.3a, GP achieves the best performance among others, and it can be observed that our method can achieve higher final average rewards compared to other baselines. In Fig.3b, baselines and the proposed method, VBO, have been tested on the Hartmann function with 6 dimensions. In this case, we again observe that GP still performs very well among other baselines, while the Infinite-width Bayesian neural network (IBNN) also achieves comparable results. Our method in this case converges faster and to a higher final average reward value. Finally, Fig.3c compares the performance of all methods on the Ackley 10 (dimension) function. In this simulation, we observe that the Sparse Gaussian method can achieve better results and higher final average reward values compared to the other baselines. Although our method first starts from lower average rewards, in the long run and next iterations, our method can still achieve higher reward values.

5.2 Experimental setup summary

To compare different algorithms, we assume a batch size of 64 for our method across Ackley and Hartmann synthetic experiments, and 32 for the Branin test function. Moreover, the learning rate for all neural networks is set to 0.002, unless otherwise specified. In Algorithm 2, we use $K_a = 1$ and $K_b = 5$. The warm-up steps varies between 20-30 in different experiments.

For neural network architectures, in all experiments, the main model is made of three fully connected (dense) layers. The helper network consists of a modified LSTM followed by two dense layers. For different baselines, we perform a grid search between various parameters of these models, and report the best performance of each method. In the Appendix, we discuss the effect of the choice of hyperparameters on final results. To compare different results, we use the average reward metric, where we compare the cumulative reward normalized by the number of iterations as a metric to compare different baselines. Moreover, for BNN baselines, a three-layer model with a ReLU activation function has been used in all baseline methods for testing on synthetic functions.

5.3 Real-world tasks and Data

Furthermore, we test our method on a real-world example. In Fig. 4a, we compare our method with other baselines on the problem of the Brusselator partial differential equation

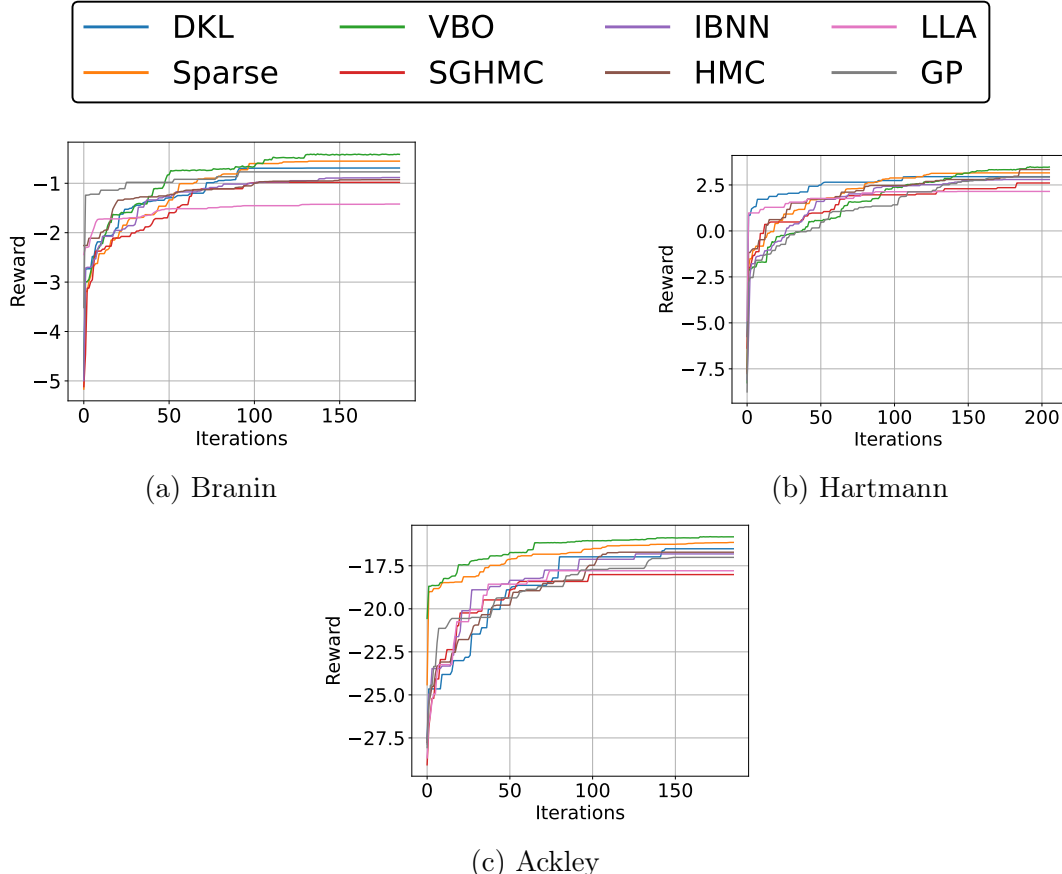


Figure 3: Comparison of the proposed method with various baselines from [29, 45] over different synthetic benchmark test functions.

optimization [29], which is the governing equation for autocatalytic reactions. In particular, in this problem, we fine-tune the four coefficients of the PDE such that the final output variance (response of the PDE or concentration of products) is minimized. Moreover, we consider the effect of replacing the Gaussian Process posterior in each term of exploitation and exploration in our acquisition function in Eq. (36). Specifically, we replace the exploration term with the Gaussian variance posterior, keep the exploitation term of Eq. (36) intact, and plot the resulting curve. Following the same idea, we have also plotted a curve where we replace the exploitation term in our proposed acquisition function with the GP mean posterior. The results are presented in Fig. 4a. The main observation here is that VBO in this scenario can achieve higher final reward values compared to other baselines. Another observation is that replacing the exploitation term in Eq. (36) with the GP posterior incurs less loss in the final reward compared to replacing the exploration term with the GP posterior. This suggests that the exploration term in the proposed acquisition function plays a central role in helping the algorithm explore better and achieve higher reward values.

In Figs. 4b, 4c, and 4d, we compare our method on other real-world tasks, including interferometer position optimization, the Lunar Lander game, and the pest control problem. The importance of considering these real-world tasks is that they represent more complex

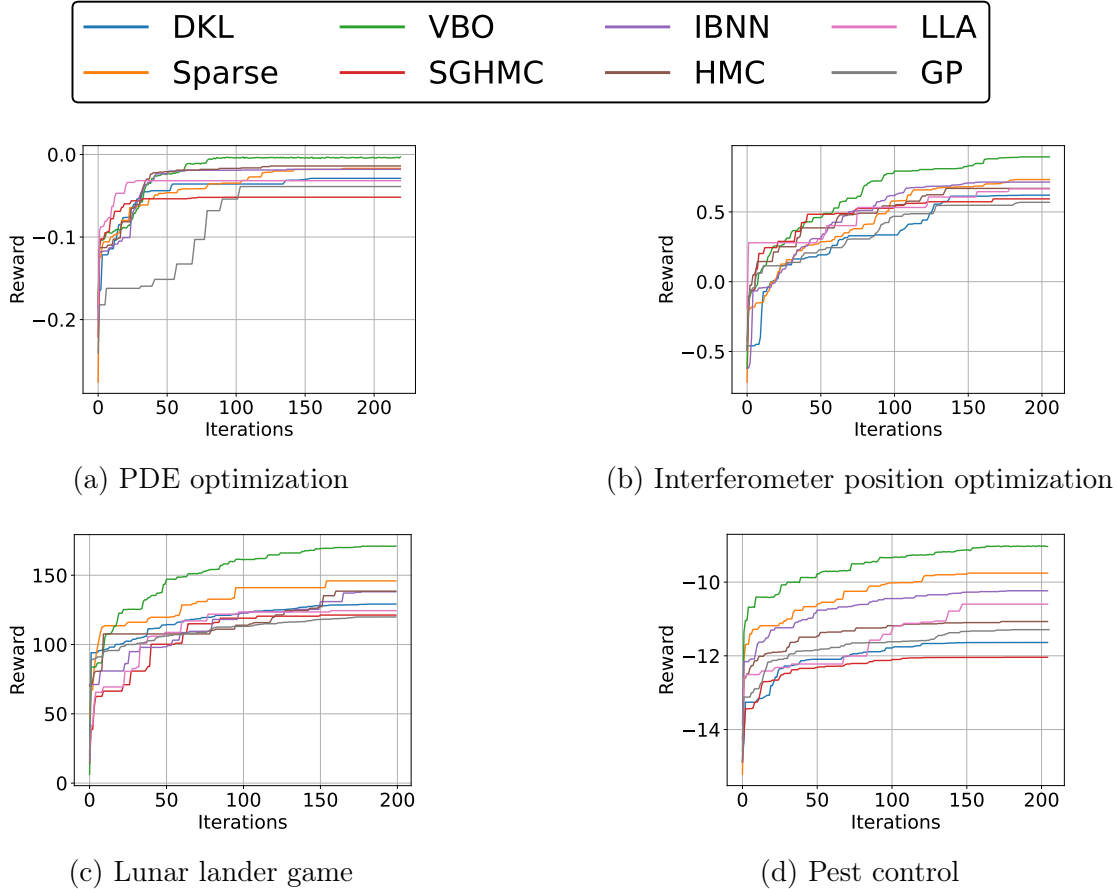


Figure 4: Comparison of the proposed method with various baselines from [29, 45] over different real-world tasks.

and higher-dimensional functions. Specifically, the interferometer task involves optimizing a 4-dimensional problem, the Lunar Lander is 12-dimensional, and the pest control problem is defined over a 25-dimensional input space. The pest control problem also involves categorical variables, each of which can take 5 values. We use a one-hot vector encoding technique [14] to apply the BO methods. To plot each method, we optimized the hyperparameters of each method to achieve the best performance. We observe that the proposed VBO method achieves superior performance compared to other baselines, especially as the dimensionality increases. Another observation is that the baseline focal sparse Gaussian method [45] usually performs better than the other baselines. Moreover, in Fig. 5 we analyze the contribution of the exploration and exploitation terms in Eq. (30) to the performance of VBO. To do so, we replace each term in turn with its counterpart derived from a GP posterior and compare the resulting performance with the full VBO. Across all four real-world tasks, we find that the exploration term is particularly critical: substituting it with a GP posterior leads to consistently lower final reward values. In other words, while replacing either term with a GP posterior reduces performance, the degradation is substantially larger when the exploration component is replaced, highlighting its key role in driving the effectiveness of VBO.

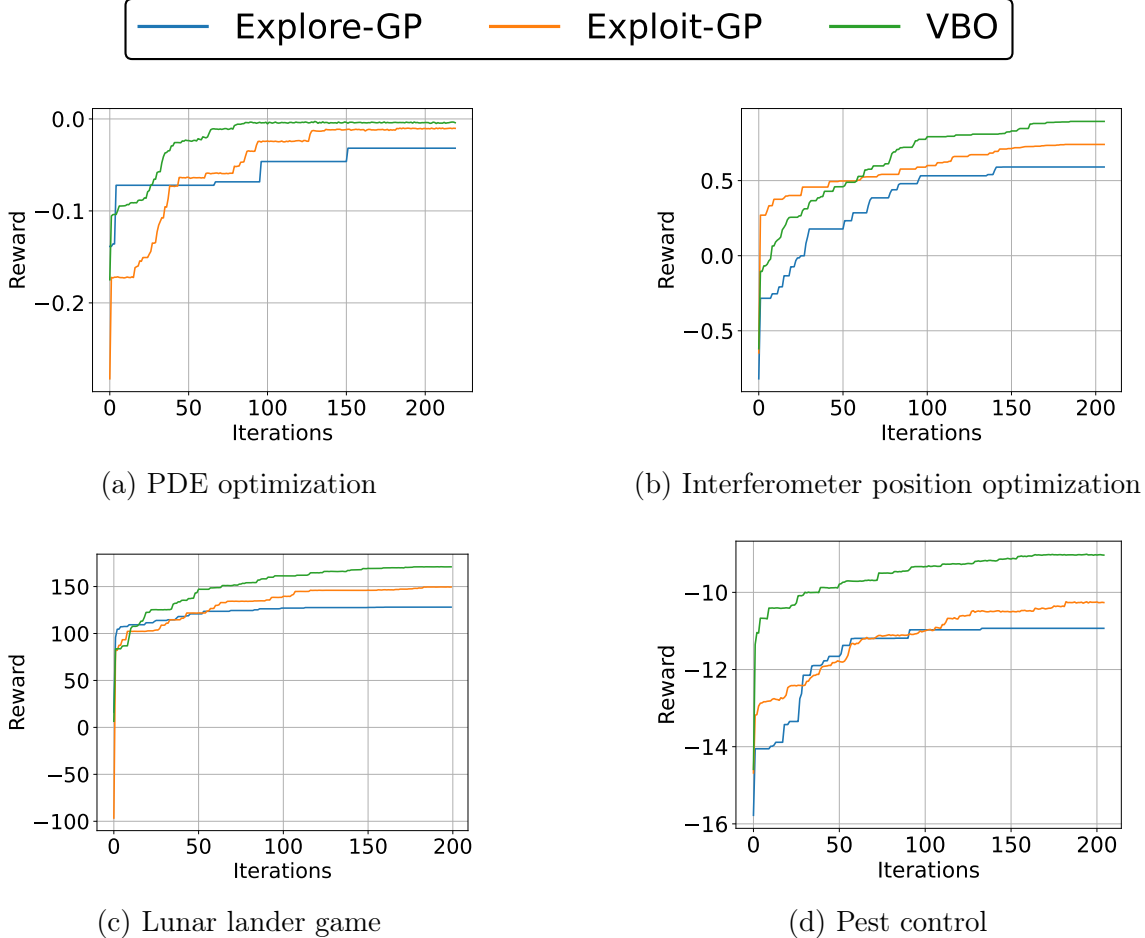


Figure 5: Impact of altering exploration and exploitation terms in Eq. (30) by substituting a GP posterior component and comparing performance with VBO.

Acknowledgments

The author would like to thank Prof. Fabrice Labeau and Dr. Hadi Shateri for the helpful discussions that has contributed to this work.

References

- [1] Miguel Aguiar, Amritam Das, and Karl H. Johansson. Universal approximation of flows of control systems by recurrent neural networks. In *2023 62nd IEEE Conference on Decision and Control (CDC)*, pages 2320–2327, 2023.
- [2] Paul H. Algoet and Thomas M. Cover. A Sandwich Proof of the Shannon-McMillan-Breiman Theorem. *The Annals of Probability*, 16(2):899 – 909, 1988.
- [3] Mohamed Ishmael Belghazi, Aristide Baratin, Sai Rajeshwar, Sherjil Ozair, Yoshua Bengio, Aaron Courville, and Devon Hjelm. Mutual information neural estimation.

In Jennifer Dy and Andreas Krause, editors, *Proceedings of the 35th International Conference on Machine Learning*, volume 80 of *Proceedings of Machine Learning Research*, pages 531–540. PMLR, 10–15 Jul 2018.

- [4] Leo Breiman. The Individual Ergodic Theorem of Information Theory. *The Annals of Mathematical Statistics*, 28(3):809 – 811, 1957.
- [5] Tianqi Chen, Emily Fox, and Carlos Guestrin. Stochastic gradient hamiltonian monte carlo. In Eric P. Xing and Tony Jebara, editors, *Proceedings of the 31st International Conference on Machine Learning*, volume 32 of *Proceedings of Machine Learning Research*, pages 1683–1691, Bejing, China, 22–24 Jun 2014. PMLR.
- [6] Nuojin Cheng, Leonard Papenmeier, Stephen Becker, and Luigi Nardi. A unified framework for entropy search and expected improvement in bayesian optimization. In *Forty-second International Conference on Machine Learning*, 2025.
- [7] T.M. Cover and J.A. Thomas. *Elements of Information Theory*. Wiley, 2012.
- [8] D.D. Cox and S. John. A statistical method for global optimization. In *[Proceedings] 1992 IEEE International Conference on Systems, Man, and Cybernetics*, pages 1241–1246 vol.2, 1992.
- [9] Zhijie Deng, Feng Zhou, and Jun Zhu. Accelerated linearized laplace approximation for bayesian deep learning. In S. Koyejo, S. Mohamed, A. Agarwal, D. Belgrave, K. Cho, and A. Oh, editors, *Advances in Neural Information Processing Systems*, volume 35, pages 2695–2708. Curran Associates, Inc., 2022.
- [10] M. D. Donsker and S. R. S. Varadhan. Asymptotic evaluation of certain markov process expectations for large time, i. *Communications on Pure and Applied Mathematics*, 28(1):1–47, 1975.
- [11] David Eriksson, Michael Pearce, Jacob Gardner, Ryan D Turner, and Matthias Poloczek. Scalable global optimization via local bayesian optimization. In H. Wallach, H. Larochelle, A. Beygelzimer, F. d'Alché-Buc, E. Fox, and R. Garnett, editors, *Advances in Neural Information Processing Systems*, volume 32. Curran Associates, Inc., 2019.
- [12] Peter I. Frazier. A Tutorial on Bayesian Optimization. *arXiv e-prints*, page arXiv:1807.02811, July 2018.
- [13] Roman Garnett. *Bayesian Optimization*. Cambridge University Press, 2023.
- [14] Eduardo C. Garrido-Merchán and Daniel Hernández-Lobato. Dealing with categorical and integer-valued variables in bayesian optimization with gaussian processes. *Neurocomputing*, 380:20–35, 2020.
- [15] James Harrison et al. Variational last layer Bayesian neural networks. In *International Conference on Learning Representations (ICLR)*, 2024.

- [16] Philipp Hennig, Michael A. Osborne, and Hans P. Kersting. *Probabilistic Numerics: Computation as Machine Learning*. Cambridge University Press, 2022.
- [17] Philipp Hennig and Christian J. Schuler. Entropy search for information-efficient global optimization. *Journal of Machine Learning Research*, 13(57):1809–1837, 2012.
- [18] Jose Miguel Hernandez-Lobato, Michael Gelbart, Matthew Hoffman, Ryan Adams, and Zoubin Ghahramani. Predictive entropy search for bayesian optimization with unknown constraints. In Francis Bach and David Blei, editors, *Proceedings of the 32nd International Conference on Machine Learning*, volume 37 of *Proceedings of Machine Learning Research*, pages 1699–1707, Lille, France, 07–09 Jul 2015. PMLR.
- [19] Kurt Hornik, Maxwell B. Stinchcombe, and Halbert L. White. Multilayer feedforward networks are universal approximators. *Neural Networks*, 2:359–366, 1989.
- [20] Hisham Husain, Vu Nguyen, and Anton van den Hengel. Distributionally robust bayesian optimization with φ -divergences. In A. Oh, T. Naumann, A. Globerson, K. Saenko, M. Hardt, and S. Levine, editors, *Advances in Neural Information Processing Systems*, volume 36, pages 20133–20145. Curran Associates, Inc., 2023.
- [21] Carl Hvarfner, Frank Hutter, and Luigi Nardi. Joint entropy search for maximally-informed bayesian optimization. In S. Koyejo, S. Mohamed, A. Agarwal, D. Belgrave, K. Cho, and A. Oh, editors, *Advances in Neural Information Processing Systems*, volume 35, pages 11494–11506. Curran Associates, Inc., 2022.
- [22] Alexander Immer, Maciej Korzepa, and Matthias Bauer. Improving predictions of bayesian neural nets via local linearization. In Arindam Banerjee and Kenji Fukumizu, editors, *Proceedings of The 24th International Conference on Artificial Intelligence and Statistics*, volume 130 of *Proceedings of Machine Learning Research*, pages 703–711. PMLR, 13–15 Apr 2021.
- [23] Masanori Ishikura and Masayuki Karasuyama. Pareto-frontier entropy search with variational lower bound maximization. In Aarti Singh, Maryam Fazel, Daniel Hsu, Simon Lacoste-Julien, Felix Berkenkamp, Tegan Maharaj, Kiri Wagstaff, and Jerry Zhu, editors, *Proceedings of the 42nd International Conference on Machine Learning*, volume 267 of *Proceedings of Machine Learning Research*, pages 26490–26522. PMLR, 13–19 Jul 2025.
- [24] Pavel Izmailov, Sharad Vikram, Matthew D Hoffman, and Andrew Gordon Gordon Wilson. What are bayesian neural network posteriors really like? In Marina Meila and Tong Zhang, editors, *Proceedings of the 38th International Conference on Machine Learning*, volume 139 of *Proceedings of Machine Learning Research*, pages 4629–4640. PMLR, 18–24 Jul 2021.
- [25] Huiwen Jia, Cong Shi, and Siqian Shen. Multi-armed bandit with sub-exponential rewards. *Operations Research Letters*, 49(5):728–733, 2021.
- [26] Felix Jimenez and Matthias Katzfuss. Scalable bayesian optimization using vecchia approximations of gaussian processes. In Francisco Ruiz, Jennifer Dy, and Jan-Willem

van de Meent, editors, *Proceedings of The 26th International Conference on Artificial Intelligence and Statistics*, volume 206 of *Proceedings of Machine Learning Research*, pages 1492–1512. PMLR, 25–27 Apr 2023.

[27] Johannes Kirschner, Ilija Bogunovic, Stefanie Jegelka, and Andreas Krause. Distributionally robust Bayesian optimization. In Silvia Chiappa and Roberto Calandra, editors, *Proceedings of the Twenty Third International Conference on Artificial Intelligence and Statistics*, volume 108 of *Proceedings of Machine Learning Research*, pages 2174–2184. PMLR, 26–28 Aug 2020.

[28] Jaehoon Lee, Jascha Sohl-dickstein, Jeffrey Pennington, Roman Novak, Sam Schoenholz, and Yasaman Bahri. Deep neural networks as gaussian processes. In *International Conference on Learning Representations*, 2018.

[29] Yucen Lily Li, Tim G. J. Rudner, and Andrew Gordon Wilson. A study of bayesian neural network surrogates for bayesian optimization. In *The Twelfth International Conference on Learning Representations*, 2024.

[30] Mitchell McIntire, Daniel Ratner, and Stefano Ermon. Sparse gaussian processes for bayesian optimization. In *Proceedings of the Thirty-Second Conference on Uncertainty in Artificial Intelligence*, UAI’16, page 517–526, Arlington, Virginia, USA, 2016. AUAI Press.

[31] Farhad Mirkarimi and Nariman Farsad. Neural computation of capacity region of memoryless multiple access channels. In *2021 IEEE International Symposium on Information Theory (ISIT)*, pages 2066–2071, 2021.

[32] Farhad Mirkarimi, Stefano Rini, and Nariman Farsad. Benchmarking neural capacity estimation: Viability and reliability. *IEEE Transactions on Communications*, 71(5):2654–2669, 2023.

[33] Samuel Müller, Noah Hollmann, Sebastian P Arango, Josif Grabocka, and Frank Hutter. PFNs: Prior-fitted networks for efficient Bayesian optimization. In *International Conference on Learning Representations (ICLR)*, 2023.

[34] XuanLong Nguyen, Martin J. Wainwright, and Michael I. Jordan. Estimating divergence functionals and the likelihood ratio by convex risk minimization. *IEEE Transactions on Information Theory*, 56(11):5847–5861, 2010.

[35] Ben Poole, Sherjil Ozair, Aaron Van Den Oord, Alex Alemi, and George Tucker. On variational bounds of mutual information. In Kamalika Chaudhuri and Ruslan Salakhutdinov, editors, *Proceedings of the 36th International Conference on Machine Learning*, volume 97 of *Proceedings of Machine Learning Research*, pages 5171–5180. PMLR, 09–15 Jun 2019.

[36] Carl Edward Rasmussen and Christopher K. I. Williams. *Gaussian Processes for Machine Learning*. The MIT Press, 11 2005.

[37] Tim G. J. Rudner, Freddie Bickford Smith, Qixuan Feng, Yee Whyte Teh, and Yarin Gal. Continual learning via sequential function-space variational inference. In Kamalika Chaudhuri, Stefanie Jegelka, Le Song, Csaba Szepesvari, Gang Niu, and Sivan Sabato, editors, *Proceedings of the 39th International Conference on Machine Learning*, volume 162 of *Proceedings of Machine Learning Research*, pages 18871–18887. PMLR, 17–23 Jul 2022.

[38] Jasper Snoek, Hugo Larochelle, and Ryan P. Adams. Practical bayesian optimization of machine learning algorithms. In *Proceedings of the 26th International Conference on Neural Information Processing Systems - Volume 2*, NIPS’12, page 2951–2959, Red Hook, NY, USA, 2012. Curran Associates Inc.

[39] Jiaming Song and Stefano Ermon. Understanding the limitations of variational mutual information estimators. In *International Conference on Learning Representations*, 2020.

[40] Jost Tobias Springenberg, Aaron Klein, Stefan Falkner, and Frank Hutter. Bayesian optimization with robust bayesian neural networks. In D. Lee, M. Sugiyama, U. Luxburg, I. Guyon, and R. Garnett, editors, *Advances in Neural Information Processing Systems*, volume 29. Curran Associates, Inc., 2016.

[41] Niranjan Srinivas, Andreas Krause, Sham Kakade, and Matthias Seeger. Gaussian process optimization in the bandit setting: No regret and experimental design. In *Proceedings of the 27th International Conference on Machine Learning*, pages 1015–1022. Omnipress, 2010.

[42] Sebastian Shenghong Tay, Chuan Sheng Foo, Urano Daisuke, Richalynn Leong, and Bryan Kian Hsiang Low. Efficient distributionally robust Bayesian optimization with worst-case sensitivity. In Kamalika Chaudhuri, Stefanie Jegelka, Le Song, Csaba Szepesvari, Gang Niu, and Sivan Sabato, editors, *Proceedings of the 39th International Conference on Machine Learning*, volume 162 of *Proceedings of Machine Learning Research*, pages 21180–21204. PMLR, 17–23 Jul 2022.

[43] Dor Tsur, Ziv Aharoni, Ziv Goldfeld, and Haim H. Permuter. Neural estimation and optimization of directed information over continuous spaces. *IEEE Transactions on Information Theory*, 69:4777–4798, 2022.

[44] Zi Wang and Stefanie Jegelka. Max-value entropy search for efficient Bayesian optimization. In Doina Precup and Yee Whyte Teh, editors, *Proceedings of the 34th International Conference on Machine Learning*, volume 70 of *Proceedings of Machine Learning Research*, pages 3627–3635. PMLR, 06–11 Aug 2017.

[45] Yunyue Wei, Vincent Zhuang, Saraswati Soedarmadji, and Yanan Sui. Scalable bayesian optimization via focalized sparse gaussian processes. In A. Globerson, L. Mackey, D. Belgrave, A. Fan, U. Paquet, J. Tomczak, and C. Zhang, editors, *Advances in Neural Information Processing Systems*, volume 37, pages 120443–120467. Curran Associates, Inc., 2024.

[46] Andrew Gordon Wilson, Zhiting Hu, Ruslan Salakhutdinov, and Eric P. Xing. Deep kernel learning. In Arthur Gretton and Christian C. Robert, editors, *Proceedings of the 19th International Conference on Artificial Intelligence and Statistics*, volume 51 of *Proceedings of Machine Learning Research*, pages 370–378, Cadiz, Spain, 09–11 May 2016. PMLR.

A Consistency Analysis of Losses

In this section, our objective is to provide theoretical guarantees for our approach based on neural networks (NN) to estimate and approximate losses L_{E_ϕ} and L_D . Specifically, we seek to prove the consistency of estimates of these losses. Consistency, in this context, refers to the property of an estimator that ensures that as the number of data points increases indefinitely, the sequence of estimates converges in probability to the true parameter. Our goal is twofold:

First, to demonstrate that the expected values can be replaced with averages using tools from the generalized Birkhoff Theorem [4] and generalized AEP theorem [2], this is not trivial since the selected actions are not independent; we cannot directly use the law of large numbers in this case (LLN). In our proofs, we follow a similar approach to other neural information estimation methods specifically, [3][43]

Second, to show that NNs can effectively approximate the underlying functions to compute these estimations using the universal approximation theorem [19]. This allows us to establish the consistency of our results. We focus on proving consistency for L_{E_ϕ} , noting that the same approach can be extended to L_{D_θ} . We do not go through all the details of proof for L_{D_θ} .

1. Estimation from samples: In the first step, we aim to demonstrate the consistency of estimating the actual loss. Specifically, we aim to show our loss:

$$\mathbb{E}[y_t \mid y_{t-1}, \dots, y_1, \mathbf{x}_{t-1}, \dots, \mathbf{x}_1] + \sqrt{\beta} \left[-\mathbb{E}_{P_{(\mathbf{X}_t, \mathbf{Y}_t)}}[D_{\theta_2}(\mathbf{X}_t, \mathbf{Y}_t)] + \log(\mathbb{E}_{P_{\mathbf{X}_t} \times P_{\mathbf{Y}_t}}[e^{D_{\theta_2}(\mathbf{X}_t, \mathbf{Y}_t)}]) \right], \quad (40)$$

can be estimated using samples:

$$L_{E_\phi} = \frac{1}{B} \sum_{i=1}^B y_t^{(i)} - \frac{1}{B} \sum_{i=1}^B D_\theta(\mathbf{x}^{(i)}, y^{(i)}) + \log \frac{1}{B^2} \sum_{i=1}^B \sum_{j=1}^B e^{D_\theta(\mathbf{x}^{(i)}, y^{(j)})}, \quad (41)$$

where $y_t^{(i)} = f(\mathbf{x}_t^{(i)}) + \epsilon_t^{(i)}$ ⁶

In our analysis, we separately consider each term in the above formulation. To establish consistency. To that end, we rely on the following two key theorems to prove our results:

Theorem A.1. *Generalized AEP (Generalized Asymptotic Equipartition Property for Markov Approximation).* [2] Let \mathcal{H} be a standard Borel space, and consider the infinite product space $\mathcal{H}_0^\infty = \prod_{t=0}^\infty \mathcal{H}$, equipped with its canonical Borel σ -algebra (Ω, \mathcal{F}) . Let \mathbb{P} represent the probability law of a stationary, ergodic stochastic process $\{X_t\}$ defined over (Ω, \mathcal{F}) , and let \mathbb{M} denote a finite-order Markov measure that has a stationary transition mechanism. Suppose that for each finite n , the n -dimensional marginal of \mathbb{P} is absolutely continuous with respect to that of \mathbb{M} , with associated joint density $p(x_0, \dots, x_{n-1})$.

Then, the generalized asymptotic equipartition property asserts that:

$$\frac{1}{n} \log p(X_0, \dots, X_{n-1}) \xrightarrow{n \rightarrow \infty} \lim_{k \rightarrow \infty} \mathbb{E} [\log p(X_k \mid X_{k-1}, \dots, X_0)]. \quad (42)$$

Generalized AEP is particularly useful when we do not have the i.i.d. assumption, and when we are dealing with a stationary ergodic process. By applying the generalized AEP for

⁶ $s_t^{(i)}$ refers to element i of random seed vector at time step t in Alg.2

the first two terms in L_{D_1} , we conclude:

$$\mathbb{E}[y_t \mid y_{t-1}, \dots, y_1, \mathbf{x}_{t-1}, \dots, \mathbf{x}_1] \rightarrow \frac{1}{B} \sum_{i=1}^B y_t^{(i)}, \quad (43)$$

$$\mathbb{E}_{P(\mathbf{x}_t, \mathbf{y}_t)}[D_{\theta_2}(\mathbf{X}_t, \mathbf{Y}_t)] \rightarrow \frac{1}{B} \sum_{i=1}^B D_{2, \theta_2}(\mathbf{x}^{(i)}, y^{(i)}). \quad (44)$$

For sample estimation of the other term in L_{E_ϕ} , we need another theorem, as noted in other works in the literature (such as [43]). As we are dealing with a function of expectation, we invoke the Generalized Birkhoff Theorem [4] to estimate

$$\log(\mathbb{E}_{P_{\mathbf{X}_t} \times P_{\mathbf{Y}_t}}[e^{D_{\theta_2}(\mathbf{X}_t, \mathbf{Y}_t)}]). \quad (45)$$

Theorem A.2. Birkhoff's Ergodic Theorem. [4]

Let (X, \mathcal{F}, μ) be a probability space, and suppose $T : X \rightarrow X$ is a measure-preserving transformation, meaning that for all $A \in \mathcal{F}$,

$$\mu(T^{-1}(A)) = \mu(A).$$

Assume $f : X \rightarrow \mathbb{R}$ is integrable with respect to μ (i.e., $f \in L^1(\mu)$).

Then the following statements hold:

1. **Almost Sure Convergence:** For μ -almost every $\mathbf{x} \in X$, the time average of f along the orbit of \mathbf{x} under T converges:

$$\lim_{n \rightarrow \infty} \frac{1}{n} \sum_{k=0}^{n-1} f(T^k(\mathbf{x})) = f^*(\mathbf{x}),$$

where f^* is a T -invariant function, meaning $f^*(T(\mathbf{x})) = f^*(\mathbf{x})$.

2. **In the Ergodic Case:** If T is ergodic (i.e., the only T -invariant sets have measure 0 or 1), then $f^*(\mathbf{x})$ is constant μ -almost everywhere and equal to the integral of f :

$$f^*(\mathbf{x}) = \int f \, d\mu \quad \text{for } \mu\text{-almost every } \mathbf{x}.$$

By the assumption of Ergodicity of input data sequences, the T transform in this case translates into the condition $\mathbb{P}(A) = \mathbb{P}(T^{-1}(A))$ for any $A \in \mathcal{F}$, where in this case we use a time-shift. By applying this to the first term, we conclude:

$$\log(\mathbb{E}_{P_{\mathbf{X}_t} \times P_{\mathbf{Y}_t}}[e^{D_{\theta_2}(\mathbf{X}_t, \mathbf{Y}_t)}]) \xrightarrow[\mathbb{P}-as]{n \rightarrow \infty} \log \frac{1}{B^2} \sum_{i=1}^B \sum_{j=1}^B e^{D_{2, \theta_2}(\mathbf{x}^{(i)}, y^{(j)})}. \quad (46)$$

By putting together all terms, we conclude:

$$\begin{aligned} & \frac{1}{B} \sum_{i=1}^B y_t^{(i)} - \frac{1}{B} \sum_{i=1}^B D_{2, \theta_2}(\mathbf{x}^{(i)}, y^{(i)}) + \log \frac{1}{B^2} \sum_{i=1}^B \sum_{j=1}^B e^{D_{2, \theta_2}(\mathbf{x}^{(i)}, y^{(j)})} \xrightarrow{n \rightarrow \infty} \\ & \mathbb{E}[y_t \mid y_{t-1}, \dots, y_1, \mathbf{x}_{t-1}, \dots, \mathbf{x}_1] - \mathbb{E}_{P(\mathbf{X}, \mathbf{Y})}[D_{2, \theta_2}(\mathbf{X}, \mathbf{Y})] + \log \mathbb{E}_{P_{\mathbf{X} \times \mathbf{Y}}}[e^{D_{2, \theta_2}(\mathbf{X}, \mathbf{Y})}]. \end{aligned} \quad (47)$$

This completes the estimation step from samples.

2. Approximation Step: Up to now, we have provided the proof for the consistent estimation of our loss. In this stage, we aim to show the possibility to approximate functional space with the space of Feed-forward network (FNN), $D_1 = \mathbf{x}_t, f(\mathbf{x}_t)$, and RNN networks, D . we apply universal approximation theorem for FNN [Theorem.2.2 [19]], and RNNs [1].

Our proof in this section is a generalization of [3, 43], as our loss has an additional term, and both feed-forward and RNN neural networks.

First, consider the first network, E_ϕ . Our aim in this part is to prove that there exists a family of feed-forward neural networks with parameter θ_1 such that:

$$|E_\phi(\mathbf{s}_t) - f(\mathbf{x}_t)| \leq \epsilon. \quad (48)$$

If we assume that the function $f(\cdot)$ is bounded from above by M , and $\epsilon \geq 0$, using corollary 2.2 of [19] we conclude there exist a neural network such that:

$$|E_{\hat{\phi}}(\mathbf{s}_t) - f(\mathbf{x}_t)| \leq \epsilon. \quad (49)$$

Now our main focus is on proving that it is possible for our "helper" network, which consists of RNNs, to approximate the functional space to find information gain between selected actions and observations. Specifically, we want to show there is an RNN with parameters θ such that:

$$|I(\mathbf{X}; \mathbf{Y}) - I_\Theta(\mathbf{X}, \mathbf{Y})| \leq \eta, \quad (50)$$

where $I_\Theta(\mathbf{X}, \mathbf{Y}) = \max_{\theta \in \Theta} (\mathbb{E}_{P_{(X,Y)}}[T_\theta(\mathbf{X}, \mathbf{Y})] - \log(\mathbb{E}_{P_{\mathbf{X} \times \mathbf{Y}}}[e^{T_\theta(X, Y)}]))$.

Based on DV representation [10]

Let: $T^*(\mathbf{X}, \mathbf{Y}) = \log \frac{p(\mathbf{X}, \mathbf{Y})}{p(\mathbf{X})p(\mathbf{Y})}$, where $\mathbf{X} = \{\mathbf{x}_t\}_{t=1}^T$, $\mathbf{Y} = \{y_t\}_{t=1}^T$ be the discriminator function for estimating information gain. Based on [1] there exist a RNN, for any $\epsilon \geq 0$ such that:

$$\sup_{\{\mathbf{x}\}_{t=1}^T, \{Y\}_{t=1}^T} |T^*(\mathbf{X}, \mathbf{Y}) - \hat{T}(\mathbf{X}, \mathbf{Y})| \leq \epsilon. \quad (51)$$

Since Eq. (51) implies $|T^*(\mathbf{X}, \mathbf{Y}) - \hat{T}(\mathbf{X}, \mathbf{Y})| \leq \epsilon \quad \forall (\mathbf{X}, \mathbf{Y})$, By applying expectation with respect to $p(\mathbf{X}, \mathbf{Y})$ we conclude:

$$|\mathbb{E}_{p(\mathbf{X}, \mathbf{Y})}[T^*(\mathbf{X}, \mathbf{Y}) - \hat{T}(\mathbf{X}, \mathbf{Y})]| \leq \epsilon. \quad (52)$$

Thus, the first term DV representation is satisfied.

Now we turn to the second term in DV representation, which is :

⁷. Now define:

$$A = \mathbb{E}_{p(\mathbf{X})p(\mathbf{Y})}[e^{T^*(\mathbf{X}, \mathbf{Y})}], \quad B = \mathbb{E}_{p(\mathbf{X})p(\mathbf{Y})}[e^{\hat{T}(\mathbf{X}, \mathbf{Y})}]. \quad (53)$$

Now it is easy to see that by using the triangular inequality, and Taylor expansion, we can find the following lower bound

$$|\log A - \log B| \leq \frac{|A - B|}{\min(A, B)}. \quad (54)$$

⁷We apply the universal approximation in the last step as a tool to prove the accurate estimation of \mathbf{x}_t , as an output of D_1 , and as result $y_t = f(\mathbf{x}_t) + \epsilon_t$

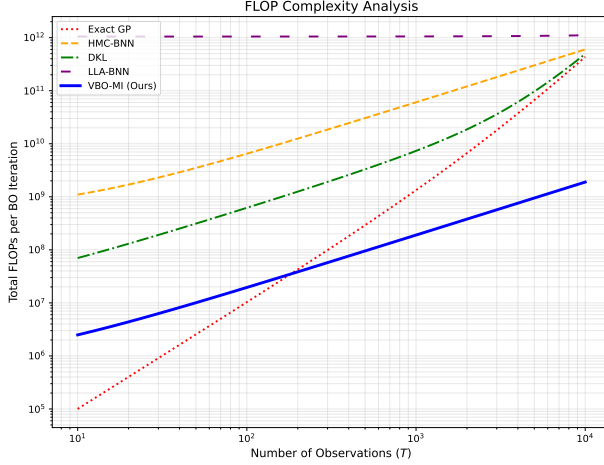


Figure 6: Theoretical computational complexity comparison measured in Floating-Point Operations (FLOPs) per Bayesian optimization iteration

Now to find the bound on $|\log A - \log B|$ we bound each term, $A - B$, and $\min(A, B)$:

If the T^* is bounded by M , e.g, $T^* \leq M$ we have:

$$|T^*(\mathbf{X}, \mathbf{Y}) - \hat{T}(\mathbf{X}, \mathbf{Y})| \leq \epsilon \implies |e^{T^*(\mathbf{X}, \mathbf{Y})} - e^{\hat{T}(\mathbf{X}, \mathbf{Y})}| \leq e^M \cdot \epsilon. \quad (55)$$

Now we turn to bound $\min(A - B)$.

If we assume that T^* is bounded from below, e.g, $T^* \geq L$, then we conclude:

$$A \geq e^L, \quad B \geq C \cdot e^L, \quad (56)$$

where $C = e^{-|\epsilon|}$. So, as \exp is monotonic, we have: $\min(A, B) \geq C \cdot e^L$.

Now, substitute the bounds for $|A - B|$ and $\min(A, B)$ in Eq. (54) to conclude:

$$|\log A - \log B| \leq \frac{e^M \cdot \epsilon}{e^{L-\epsilon}} = e^{M-L+\epsilon} \cdot \epsilon. \quad (57)$$

Since e^{M-L} is bounded, as $\epsilon \rightarrow 0$:

$$|\log A - \log B| \leq \mathcal{O}(\epsilon) \rightarrow 0. \quad (58)$$

By combining Eq. (52), and Eq. (58) we conclude Eq. (50). Now by combining Eq. (49), and Eq. (50) we conclude that estimation and approximation of L_{E_ϕ} is consistent. As L_{D_2} has similar terms to L_{E_ϕ} , the proof is similar and we omit the details here.

B Experimental Setups

To ensure a fair comparison with previously reported results, we adopt the same benchmark problems and hyperparameter configurations as described in the referenced study, applied to the following four experimental scenarios: *Lunar Lander*, *PDE Optimization*, *Interferometer Design*, and *Pest Control*. The setup and tuning parameters are summarized below.

Lunar Lander — The objective is to learn an optimal control policy for the OpenAI Gym `LunarLander-v2` environment. The reward function is computed over full episodes, and the goal is to maximize the expected return. The policy is modeled as a feed-forward neural network with two hidden layers of size 256 using `tanh` activations. A learning rate of 3×10^{-4} is used with the Adam optimizer. The search space for controller parameters is restricted to a fixed range around zero, and the evaluation budget matches that of the baseline study.

PDE Optimization — This problem involves identifying an optimal coefficient field for a partial differential equation defined over a two-dimensional domain, intending to minimize the mismatch between simulated and target solutions. The domain is discretized into a 32×32 grid, and the coefficients are parameterized by a neural network with two hidden layers of width 100. Optimization is performed using a learning rate of 1×10^{-3} and the Adam optimizer. The PDE solver is run with fixed boundary conditions and the same spatial resolution as in the baseline experiments.

Interferometer Position optimization — The task here is to configure an optical interferometer for maximum sensitivity in a specified frequency range. The design variables represent mirror positions and phase shifts. The parameter vector has dimension 4 and is optimized within the specified physical limits. A feedforward network with three hidden layers of size 128 is employed, using `ReLU` activations, a learning rate of 1×10^{-3} , and the Adam optimizer as a BNN neural network.

Pest Control — This benchmark focuses on adjusting a policy to control the dynamics of the pest population over multiple seasons. The environment is modeled as a stochastic dynamical system with discrete-time steps. The policy is parameterized by a two-layer neural network with 128 neurons per layer and `tanh` activations. The optimizer is Adam with a learning rate of 2×10^{-3} . The search space is restricted to feasible application rates, ensuring the policy remains biologically viable. For all experiments, Bayesian Optimization is performed with an initial design of n_{init} points followed by sequential acquisition steps until the total evaluation budget is reached. The acquisition function and other algorithm-specific parameters follow the original study for comparability. Reported results are averaged over multiple random seeds to account for stochastic variability.

C Computational Complexity and FLOP Analysis

A significant bottleneck in Bayesian optimization is the computational overhead associated with surrogate model updates and the inner-loop optimization of the acquisition function. We evaluate the complexity of our proposed VBO-MI framework in terms of Floating-Point Operations (FLOPs) and compare it against standard BNN-based surrogates: Hamiltonian Monte Carlo (HMC), Deep Kernel Learning (DKL), and Linearized Laplace Approximation (LLA).

Surrogate Update Complexity. For a dataset of size T and a model with W parameters, the HMC method is the most computationally demanding. It requires S posterior samples, where each sample involves L leapfrog steps. Each step requires a full gradient evaluation over T , leading to a complexity of $\mathcal{O}(S \cdot L \cdot T \cdot W)$. DKL involves an $O(T^3)$ Cholesky decomposition in addition to neural network training. In contrast, our VBO-MI framework

utilizes a "Helper" LSTM network. The update cost is $\mathcal{O}(K_a \cdot T \cdot H)$, where H represents the LSTM hidden state dimension and K_a is the number of gradient steps. Since $K_a \ll (S \cdot L)$, our method achieves a significant reduction in FLOPs during the training phase.

Acquisition Optimization Bottleneck. In traditional BO, selecting the next point requires an auxiliary optimizer (e.g., L-BFGS) to maximize the acquisition function $\alpha(\mathbf{x})$. For BNNs, this requires averaging forward passes over S ensemble members for every candidate point x evaluated by the optimizer. If the optimizer takes N_{steps} with N_{starts} restarts, the cost is $\mathcal{O}(N_{starts} \cdot N_{steps} \cdot S \cdot W)$.

Our Action-net (E_ϕ) bypasses this "inner-loop" optimization. By maintaining a differentiable mapping from a random seed to the input space, we select the next point through K_b direct gradient updates on the network parameters ϕ . This amortizes the search cost, reducing the acquisition complexity to $\mathcal{O}(K_b \cdot W)$. As shown in Table 1, this result in a near $10^2 \times$ reduction in FLOPs for the acquisition phase compared to sampling-based BNNs.

Fig. 6 illustrate the complexity comparisons among different methods. Although both HMC-BNN and VBO-MI scale linearly with the number of observations T , our framework maintains a substantially lower constant factor due to the elimination of the leapfrog integration loop and the auxiliary acquisition optimizer.

Table 1: Comparison of FLOP complexity per BO iteration. T : observations, W : weights, S : samples, L : leapfrog steps, $K_{a,b}$: variational update steps. We assume $W > H$ and $S, L > K_{a,b}$.

METHOD	SURROGATE UPDATE	ACQUISITION OPT.	SCALING
GP (EXACT)	$\mathcal{O}(T^3)$	$N \cdot \mathcal{O}(T^2)$	CUBIC
HMC-BNN	$\mathcal{O}(S \cdot L \cdot T \cdot W)$	$N \cdot \mathcal{O}(S \cdot W)$	HIGH LINEAR
DKL	$\mathcal{O}(T \cdot W + T^3)$	$N \cdot \mathcal{O}(T^2 + W)$	CUBIC
LLA	$\mathcal{O}(T \cdot W + W^3)$	$N \cdot \mathcal{O}(W^2)$	LINEAR
VBO-MI (OURS)	$\mathcal{O}(K_a \cdot T \cdot H)$	$\mathcal{O}(K_b \cdot W)$	LOW LINEAR

D Additional Numerical Evaluations

In this section, we provide additional numerical results and an evaluation of our method and its comparison with several baselines.

Specifically, we consider the final converged value of each method and its variance for each four real-world tasks considered earlier. These evaluations are presented in Table. 3 to 6. Moreover, we consider the effect of bath size on the final result of each baseline and VBO on all four real-world tasks. The results are shown in Fig. 7. Finally, we consider the sensitivity of our proposed method to the parameter β , and compare it to other methods in various real-world tasks in Fig. 8. In this context, by sensitivity, we mean how much the final convergent reward value changes with various values of the parameter β . Our main conclusion here is that VBO is less sensitive to the choice of parameter β compared to other methods

Table 2: Parameters and constants used for the theoretical FLOP complexity analysis in Section C. These values represent a standard configuration for a small-to-medium scale Bayesian Neural Network surrogate in a black-box optimization setting.

PARAMETER	VALUE	DESCRIPTION
W	10,000	TOTAL NUMBER OF BNN PARAMETERS (WEIGHTS AND BIASES)
D	10	INPUT DIMENSIONALITY OF THE OBJECTIVE FUNCTION
H	64	HIDDEN STATE DIMENSION OF THE VARIATIONAL CRITIC (LSTM)
S	50	NUMBER OF POSTERIOR SAMPLES (FOR HMC)
L	20	LEAPFROG STEPS PER HMC SAMPLE
E	100	EPOCHS FOR INITIAL SURROGATE FITTING (DKL/LLA)
N_{STARTS}	10	RESTARTS FOR ACQUISITION FUNCTION OPTIMIZATION
N_{STEPS}	50	ITERATIONS PER RESTART FOR ACQUISITION OPTIMIZATION
K_a	5	GRADIENT UPDATE STEPS FOR THE VARIATIONAL CRITIC
K_b	10	GRADIENT UPDATE STEPS FOR THE ACTION-NET

and can achieve higher reward values across multiple hyperparameters β . Moreover, we find that usually with a larger batch size of data, the performance of VBO can be improved up to a threshold.

Table 3: PDE-Average over the last 20 iterations

Method	Final Reward	Variance ($\times 10^{-5}$)
VBO with GP exploration	-0.0293	0.010
VBO with GP exploitation	-0.011	0.003
DKL	-0.0289	0.001
Sparse	-0.0175	0.032
HMC	-0.0139	0.001
GP	-0.0349	0.030
VBO	-0.0071	0.007
IBNN	-0.018	0.001
LLA	-0.031	0.001
SGHMC	-0.051	0.001

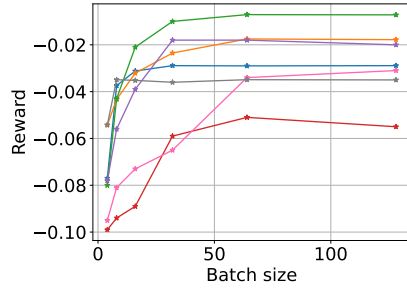
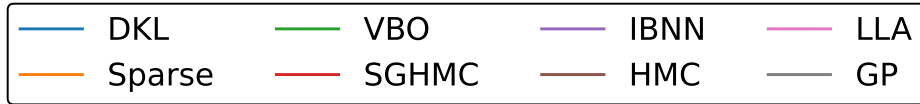
Table 4: Lunar Lander- Average over the last 20 iterations

Method	Final Reward	Variance ($\times 10^{-2}$)
VBO with GP exploration	128.07	0.0100
VBO with GP exploitation	149.33	0.1500
DKL	129.17	0.0200
Sparse	145.9	0.0700
HMC	138.51	0.0010
GP	119.88	0.0030
VBO	170.97	0.0500
IBNN	138.07	0.0010
LLA	124.45	0.0010
SGHMC	121.25	0.0010

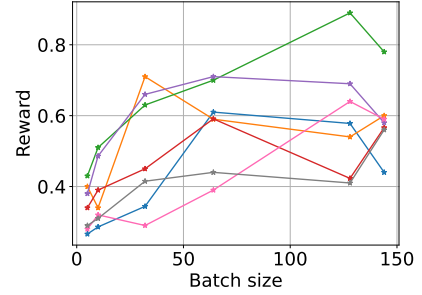
Table 5: Pest Control- Average over the last 20 iterations

Method	Final Reward	Variance ($\times 10^{-4}$)
VBO with GP exploration	-10.93	0.0160
VBO with GP exploitation	-10.27	0.1490
DKL	-11.63	0.0010
Sparse	-9.75	0.0070
HMC	-11.08	0.0001
GP	-11.30	0.0030
VBO	-9.02	0.0350
IBNN	-10.244	0.0090
LLA	-10.59	0.0001
SGHMC	-12.04	0.0

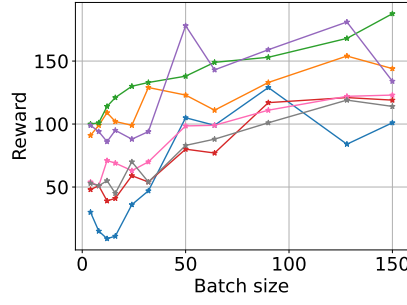
Batch size effect on results



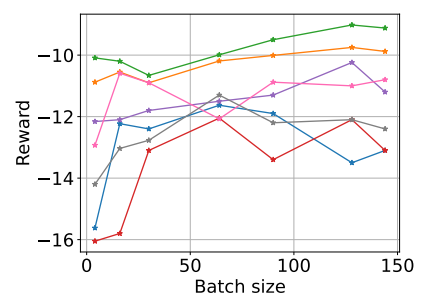
(a) PDE optimization



(b) Interferometer position optimization



(c) Lunar lander game



(d) Pest control

Figure 7: Comparison of various baselines with VBO at different batch sizes of data

Table 6: Interferometer- Average over the 20 last iterations

Method	Final Reward	Variance ($\times 10^{-1}$)
VBO with GP exploration	0.379	0.0730
VBO with GP exploitation	0.586	0.0230
DKL	0.619	0.0007
Sparse	0.730	0.0039
HMC	0.668	0.0003
GP	0.567	0.0030
VBO	0.890	0.0006
IBNN	0.710	0.0001
LLA	0.664	0.0021
SGHMC	0.590	0.0001

Beta (β) effect on results

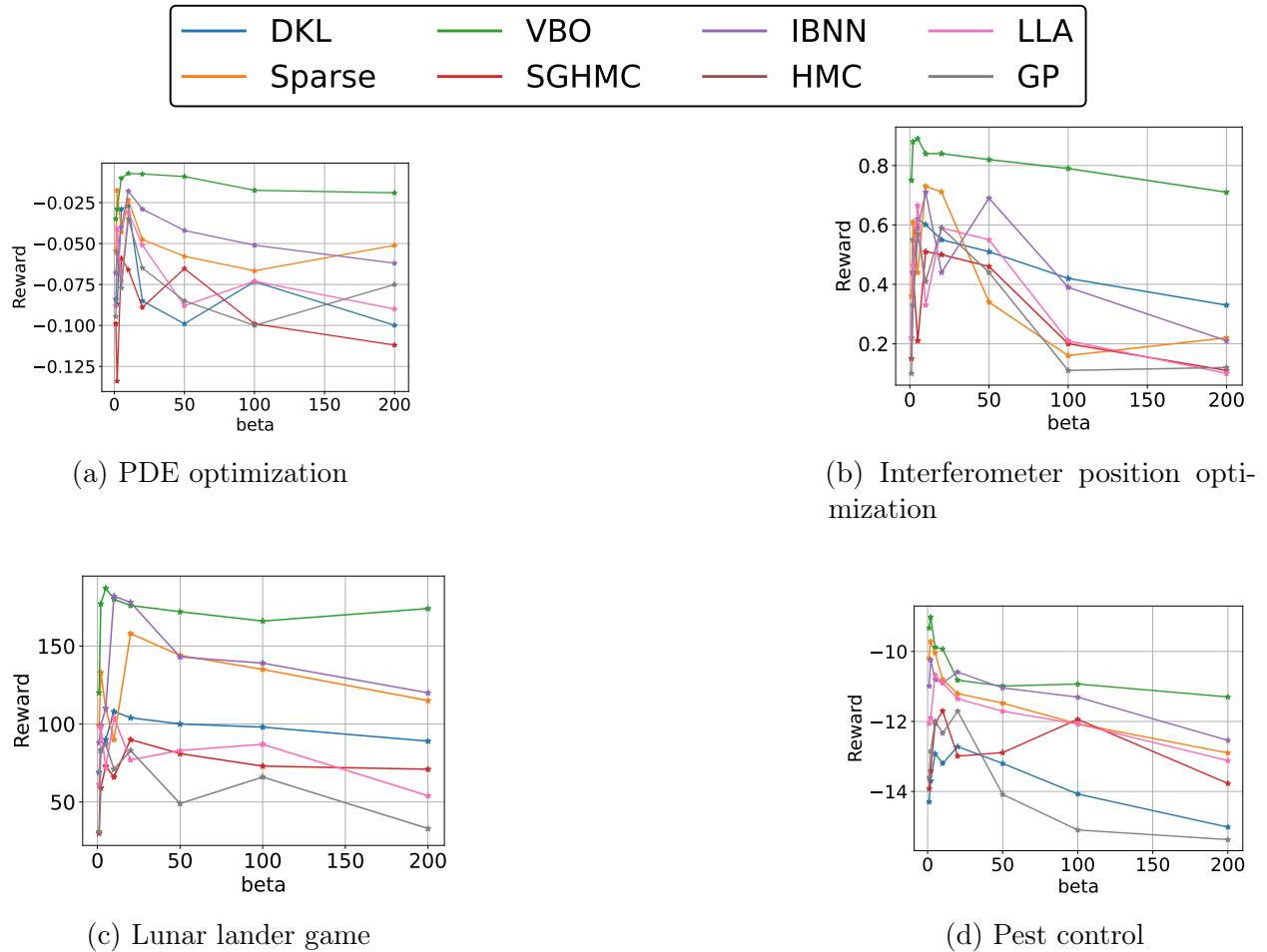


Figure 8: Comparison of various baselines with VBO at different beta values when GP-UCB is used as acquisition function for all methods.